The Catalytic Properties of Murine Carbonic Anhydrase VII†

J. Nicole Earnhardt,‡ Minzhang Qian,§ Chingkuang Tu,§ Maha M. Lakkis,|| Nils C. H. Bergenhem,⊥ Philip J. Laipis,‡ Richard E. Tashian,# and David N. Silverman*,§

Department of Biochemistry and Molecular Biology and Department of Pharmacology and Therapeutics, University of Florida, Gainesville, Florida 32610, and Department of Human Genetics, University of Michigan Medical School, Ann Arbor, Michigan 48109

Received January 7, 1998; Revised Manuscript Received May 19, 1998

ABSTRACT: Carbonic anhydrase VII (CA VII) appears to be the most highly conserved of the active mammalian carbonic anhydrases. We have characterized the catalytic activity and inhibition properties of a recombinant murine CA VII. CA VII has steady-state constants similar to two of the most active isozymes of carbonic anhydrase, CA II and IV; also, it is very strongly inhibited by the sulfonamides ethoxzolamide and acetazolamide, yielding the lowest K_i values measured by the exchange of ^{18}O between CO_2 and water for any of the mammalian isozymes of carbonic anhydrase. The catalytic measurements of the hydration of CO_2 and the dehydration of HCO_3^- were made by stopped-flow spectrophotometry and the exchange of ^{18}O using mass spectrometry. Unlike the other isozymes of this class of CA, for which k_{cat}/K_m is described by the single ionization of zinc-bound water, CA VII exhibits a pH profile for k_{cat}/K_m for CO_2 hydration described by two ionizations at pK_a 6.2 and 7.5, with a maximum approaching 8×10^7 M^{-1} s^{-1}. The pH dependence of k_{cat}/K_m for the hydrolysis of 4-nitrophenyl acetate could also be described by these two ionizations, yielding a maximum of 71 M^{-1} s^{-1} at pH >9. Using a novel method that compares rates of ^{18}O exchange and dehydration of HCO_3^-, we assigned values for the apparent pK_a at 6.2 to the zinc-bound water and the pK_a of 7.5 to His 64. The magnitude of k_{cat}, its pH profile, ^{18}O-exchange data for both wild-type and a H64A mutant, and inhibition by $CuSO_4$ and acrolein suggest that the histidine at position 64 is functioning as a proton-transfer group and is responsible for one of the observed ionizations. A truncation mutant of CA VII, in which 23 residues from the amino-terminal end were deleted, has its rate constant for intramolecular proton transfer decreased by an order of magnitude with no change in k_{cat}/K_m. This suggests a role for the amino-terminal end in enhancing proton transfer in catalysis by carbonic anhydrase.

The mammalian carbonic anhydrases are monomeric zinc metalloenzymes that catalyze the hydration of carbon dioxide to form bicarbonate and a proton. The enzymatic mechanism has been well studied in the α-class of carbonic anhydrases which includes seven functional mammalian isozymes (*1*). Catalysis occurs in two stages; the first involves the conversion of CO_2 to HCO_3^- with the zinc-bound hydroxide participating in the catalysis (eq 1). The second stage requires proton transfer from enzyme to buffer in solution (designated as B in eq 2) to regenerate the zinc-bound hydroxide (*2*, *3*). This proton transfer has been shown in carbonic anhydrase II to proceed through intramolecular proton transfer to an active site residue, His 64 (designated as H^+E), which subsequently releases the proton to solution (*4*, *5*). The high rate of catalysis of the hydration of CO_2 [near 10^6 s^{-1} for isozyme II (*6*)] is determined almost entirely by the intramolecular proton transfer between His 64 and the zinc-bound water (*7*, *8*).

$$CO_2 + EZnOH^- \rightleftarrows EZnHCO_3^- \overset{+H_2O}{\rightleftharpoons} HCO_3^- + EZnH_2O \quad (1)$$

$$EZnH_2O + B \rightleftarrows H^+EZnOH^- + B \rightleftarrows EZnOH^- + BH^+ \quad (2)$$

A human CA VII[1] gene was isolated from a genomic library using a mouse CA II cDNA clone as a probe (*9*). The gene structure of CA VII is very similar to the other functional isozymes, and CA VII is postulated to be a cytosolic enzyme (*9*). Phylogenetic analysis of the CA isozymes places CA VII closest to the mitochondrial CA V isozyme (*1*). This is further supported by the mapping of both CA V and CA VII genes to human chromosome 16 (*9*,

† This work was supported by Grants GM25154 (D.N.S.) and GM24681 (R.E.T.) from the National Institutes of Health.

* Address correspondence to this author at Box 100267 Health Center, University of Florida College of Medicine, Gainesville, FL 32610-0267. Telephone: (352) 392-3556. FAX: (352) 392-9696. E-mail: silvrmn@nervm.nerdc.ufl.edu.

‡ Department of Biochemistry and Molecular Biology, University of Florida.

§ Department of Pharmacology and Therapeutics, University of Florida.

|| Current address: Department of Medicine, Cardiology Division, 809 Stellar-Chance Labs, University of Pennsylvania Medical School, Philadelphia, PA 19130-1600.

⊥ Current address: Novo Nordisk A/S, Department of Vessel Wall Biology, Biochemistry, Hagedornsvej 1, HAB 1.106, DK-2820 Gentofte, Denmark.

Department of Human Genetics, University of Michigan.

S0006-2960(98)00046-4 CCC: $15.00 © 1998 American Chemical Society
Published on Web 07/09/1998

10). CA VII mRNA has been detected in baboon salivary gland (*9*) and rat lung (*11*). A recent detailed in situ hybridization study of CA VII mRNA expression in adult mouse brain revealed a wide, nonspecific distribution in different regions of the cerebrum and cerebellum (*12*). CA VII has also been reported from a cDNA library prepared from multiple sclerosis lesions found in a human patient (GenBank Accession No. N78377).

Human and mouse sequence comparisons on a nearly complete mouse CA VII cDNA obtained by RT-PCR using RNA isolated from adult mouse (C57/BL6) brain showed a protein sequence identity between the two isozymes of about 95%; the nucleotide sequences are about 91% identical (*13*). The structural organization of the consensus active-site residues of the high-activity CA II isozymes is generally considered to be closest to the ancestral state. However, when selected amino acid residues (inferred to line the active-site cavity) from both active CA isozymes and inactive CA isoforms are compared to the corresponding residues of human CA II and CA VII, it is CA VII rather than CA II that seems to show the greater residue identity (*1*). This suggests that the active site of CA VII more nearly resembles that of the ancestral active site and makes CA VII the most highly conserved of any of the active CA isozymes (see Table 10 in ref *1*). This evolutionary conservation, together with the fact that CA VII is seemingly expressed in a wide variety of tissues albeit at low levels, suggests that it may have an important general function in most cells. For this reason, a study of its kinetic properties is well worth investigating.

Initial kinetic characterization of the expressed recombinant murine CA VII demonstrated an isozyme with rather low CO_2 hydration activity between pH 6.5 and 8.2 when compared to bovine CA II (*14*). Here we report a complete kinetic characterization of CA VII determined by stopped-flow spectrophotometry, ^{18}O exchange using mass spectrometry at chemical equilibrium, hydrolysis of 4-nitrophenyl acetate, and inhibition by two sulfonamides, $CuSO_4$, and acrolein. The results of these studies show a high-activity enzyme with the maximal values of k_{cat}/K_m and k_{cat} for CO_2 hydration approaching that of CA II, placing it in the subset of rapidly acting carbonic anhydrases that includes isozymes II and IV. Similar to murine CA IV (*15*), evidence indicates that CA VII shows multiple intramolecular proton transfer involving the zinc-bound water and at least two residues that act as proton shuttles, one of which is His 64. Combining data from ^{18}O exchange and stopped flow, the apparent pK_a values of His 64 and the zinc-bound water were assigned. CA VII has the strongest inhibition by the sulfonamides acetazolamide and ethoxzolamide for any carbonic anhydrase in the α class. Finally, a truncation mutant of CA VII lacking 23 residues at the amino-terminal end showed intramolecular proton transfer decreased by an order of magnitude while k_{cat}/K_m was unchanged, suggesting a role for the amino-terminal end in proton transfer to the active site.

MATERIALS AND METHODS

Expression and Purification of a Recombinant Murine CA VII cDNA. An almost entire recombinant murine CA VII cDNA (rMCA VII) was obtained by RT-PCR using RNA isolated from adult mouse (C57/BL6) brain. The PCR fragment was amplified using a human CA VII 5′ primer and a mouse CA VII 3′ primer (see Figure 1); it was cloned into the glutathione *S*-transferase expression vector pGEX.KG, a derivative of pGEX-2T (*14*, *16*). The resulting plasmid, pGEXmCA7, was transformed into *Escherichia coli* (DH5α) and rMCA VII protein expressed and purified as follows (*14*, *16*, *17*). IPTG was added to a final concentration of 0.4 mM to induce expression of rMCA VII in DH5α cells grown in 2 × YT medium (with ampicillin). Frozen DH5α cells containing the expressed rMCA VII were thawed in a solution of PBST containing 2 mM EDTA, 0.2 mM phenylmethanesulfonyl fluoride, 5 mM benzamidine, 0.4 mM $MgCl_2$, 0.4 mM $ZnSO_4$, 0.1% β-mercaptoethanol, 0.1 mg/mL deoxyribonuclease I, and 0.5 mg/mL lysozyme with stirring for 2 h at 4 °C. After cell lysis, the cell debris was pelleted by centrifugation at 23000*g* for 1 h at 4 °C. The supernatant was subjected to two affinity chromatography steps. First, the supernatant containing the glutathione *S*-transferase/rMCA VII fusion protein was stirred with 10 mL of swollen glutathione *S*-agarose beads (Sigma Chemical Co.), equilibrated in PBST at 4 °C to allow binding of the fusion protein to the beads. The beads were washed with cold PBST, and 20 mL of thrombin cleavage buffer (50 mM Tris, pH 8.0, 150 mM NaCl, 2.5 mM $CaCl_2$, and 0.1% β-mercaptoethanol) was added to equilibrate the beads for thrombin cleavage. Thrombin cleavage of the fusion protein was achieved by the addition of 10 units of thrombin in thrombin cleavage buffer and incubation at room temperature for 30 min. rMCA VII was collected in the eluate and dialyzed against 1 mM Tris (pH 8.0). The second purification step involved affinity chromatography on a gel containing *p*-aminomethylbenzenesulfonamide coupled to agarose beads according to Khalifah et al. (*18*) with minor modifications. The enzyme was then stored at 4 °C, but could also be stored at −20 or −70 °C with 100% recovery of original activity.

Subcloning and Site-Directed Mutagenesis of CA VII. Oligonucleotides which introduced (1) an *Nde*I restriction site containing a methionine codon at position 998 in pGEXmCA7, changing the Pro (CCC) codon at cDNA amino acid position 23 to a Met codon (CACAAAGCTGCATATGATTGCCCAGGG), and (2) a *Bcl*I restriction site (including the natural stop codon) at position 1728 in pGEXmCA7 (ATGGAGTCTTGATCAGGCCTGGAA) were synthesized and used in four separate PCR reactions to amplify the truncated form of murine CA VII (MCA VIIb). This truncation removes the first 23 amino acids of the original rMCA VII cDNA. The products of the PCR reactions were cloned into pGEM-T (Promega) and four independent clones from the separate PCR reactions sequenced. Two clones (all four contained the correct sequence) were then mutated using single-stranded DNA template and a mutating oligonucle-

[1] Abbreviations: CA, carbonic anhydrase; rMCA VII, recombinant murine carbonic anhydrase VII; MCA VIIb, a truncated form of murine carbonic anhydrase VII lacking 23 residues from the amino-terminal end; Mes, 2-(*N*-morpholino)ethanesulfonic acid; Mops, 3-(*N*-morpholino)propanesulfonic acid; Hepes, *N*-(2-hydroxyethyl)piperazine-*N*′-2-ethanesulfonic acid; Taps, 3-[tris(hydroxymethyl)methyl]amino-propanesulfonic acid; Ches, 2-(cyclohexylamino)ethanesulfonic acid; IPTG, isopropyl β-D-thiogalactoside; PBST, solution containing 150 mM NaCl, 16 mM Na_2HPO_4, 4 mM NaH_2PO_4, pH 7.3, and 1% Triton X-100; SHIE, solvent hydrogen isotope effect.

otide (AGAGGATTCACATGGTGGACA) to remove the naturally occurring *Nde*I site at position 724 in the rMCA VII cDNA insert (*19*). The mutated inserts were removed from pGEM-T by digestion with *Nde*I and *Bcl*I and inserted into a *Nde*I and *Bam*HI-cleaved pET31+ expression vector (*20*) to allow efficient high-level expression and site-directed mutagenesis. Construction of the His64Ala mutant form of MCA VIIb was as previously described (*19*, *20*). The various forms of MCA VIIb were expressed in *E. coli* strain BL21(DE3)pLysS as described (*20*). DNA from the expression plasmids used to produce each of the different forms of MCA VIIb was sequenced to confirm the structure of each insert. Four consistent silent mutations were found at third codon positions in all sequenced plasmids compared to the original published sequence (*13*).

Purification of the MCA VIIb proteins was performed according to previously described procedures using affinity chromatography on a gel containing *p*-aminomethylbenzenesulfonamide coupled to agarose beads (*18*, *21*). The enzyme was then stored at 4 °C.

Enzyme Purity. Electrophoresis on a 10% polyacrylamide gel stained with Coomassie Blue was used to confirm the purity of all of the CA VII enzyme samples. All enzyme samples used in the kinetic experiments were greater than 95% pure. Active CA VII enzyme concentration was determined by inhibitor titration of the active site with ethoxzolamide (K_i = 0.5 nM) by measuring ^{18}O exchange between CO_2 and water (see below). The molar absorptivity at 280 nm was determined to be 2.6×10^4 M^{-1} cm^{-1} for the rMCA VII.

Formylethylation of Full-Length CA VII. Purified full-length rMCA VII was chemically modified by acrolein to formylethylate a maximal number of exposed histidine and lysine residues and possibly cysteine residues. We followed the procedure of Pocker and Janjíc (*22*) in which 15 μM CA VII was reacted for about 4 h with a 300-fold molar excess of acrolein in solutions at room temperature containing 50 mM Ches buffer at pH 9. The reaction mixture was then extensively dialyzed.

Stopped-Flow Spectrophotometry. Initial velocities were determined by following the change in absorbance of a pH indicator (*6*) at 25 °C using a stopped-flow spectrophotometer (Applied Photophysics Model SF.17MV). CO_2 solutions were made by bubbling carbon dioxide into water or D_2O for the solvent hydrogen isotope effect studies. Dilutions were made through two syringes with a gastight connection. The CO_2 concentrations for the substrates ranged from 1.7 to 17 mM in H_2O. For the dehydration direction, $KHCO_3$ was dissolved in degassed water, and the HCO_3^- substrate concentrations ranged from 2.8 to 25 mM in H_2O. Final buffer concentrations were 25 mM, and Na_2SO_4 was used to achieve a final ionic strength of 0.2 M. The buffer−indicator pairs, the pK_a values, and the wavelengths observed were as follows: Mes (pK_a = 6.1) and chlorophenol red (pK_a = 6.3), 574 nm; Mops (pK_a = 7.2) and *p*-nitrophenol (pK_a = 7.1), 401 nm; Hepes (pK_a = 7.5) and phenol red (pK_a = 7.5), 557 nm; Taps (pK_a = 8.4) and *m*-cresol purple (pK_a = 8.3), 578 nm; Ches (pK_a = 9.3) and thymol blue (pK_a = 8.9), 596 nm. For each substrate at each pH, the mean initial velocity was determined with at least six traces of the initial 5−10% of the reaction. The uncatalyzed rates were determined in a similar manner and subtracted from the total observed rates. The kinetic constants, k_{cat}, and k_{cat}/K_m and the determination of apparent ionization constants from their pH profiles were carried out by nonlinear least-squares methods using Enzfitter (Elsevier-Biosoft). Standard errors in k_{cat} and k_{cat}/K_m were generally in the range of 5−20% and 1−10%, respectively.

^{18}O Exchange. The rate of exchange of ^{18}O between species of CO_2 and water (eqs 3 and 4) is catalyzed by carbonic anhydrase (*23*):

$$HCOO^{18}O^- + EZnH_2O \rightleftarrows EZnHCOO^{18}O^- + H_2O \rightleftarrows COO + EZnO^{18}H^- + H_2O \quad (3)$$

$$EZnO^{18}H^- + BH^+ \rightleftarrows H^+EZn^{18}OH^- + B \rightleftarrows EZnH_2{}^{18}O \xrightleftharpoons{+H_2O} EZnH_2O + H_2{}^{18}O \quad (4)$$

Using an Extrel EXM-200 mass spectrometer with a membrane permeable to gases, we measured the exchanges of ^{18}O shown in eqs 3 and 4 at chemical equilibrium and 25 °C (*23*). Solutions used no added buffers while maintaining a total ionic strength of 0.2 M with Na_2SO_4 unless otherwise indicated.

This method determines two rates in the catalytic pathway (*23*). The first is R_1, the rate of interconversion of CO_2 and HCO_3^- at chemical equilibrium. Equation 5 shows the substrate dependence of R_1.

$$R_1/[E] = k_{cat}{}^{ex}[S]/(K_{eff}{}^{S} + [S]) \quad (5)$$

Here [E] is the total enzyme concentration, $k_{cat}{}^{ex}$ is a rate constant for maximal HCO_3^- to CO_2 interconversion, [S] is the substrate concentration of HCO_3^- and/or CO_2, and $K_{eff}{}^{S}$ is an apparent substrate binding constant (*24*). Equation 5 can be used to determine the values of $k_{cat}{}^{ex}/K_{eff}{}^{S}$ when applied to the data for varying substrate concentrations, or to determine $k_{cat}{}^{ex}/K_{eff}{}^{S}$ directly from R_1 when $[S] \ll K_{eff}{}^{S}$. In the studies reported here, the values of $R_1/[E]$ as a function of the total concentration of all species of CO_2 were linear up to $([CO_2] + [HCO_3^-]) = 200$ mM. This indicates that $[S] \ll K_{eff}{}^{S}$, and under this condition $k_{cat}{}^{ex}/K_{eff}{}^{S}$ can be obtained directly from $R_1/[E]$. Under steady-state conditions, when $[S] \ll K_m$, all enzyme species are at their equilibrium concentrations. Hence, in both theory and practice, $k_{cat}{}^{ex}/K_{eff}{}^{CO_2}$ is equivalent to k_{cat}/K_m for CO_2 hydration as measured by steady-state methods (*23*, *24*). The kinetic constant k_{cat}/K_m and the determination of apparent ionization constants from the pH profile were carried out by nonlinear least-squares methods using Enzfitter (Elsevier-Biosoft).

This method also determines a second rate which is the rate of release from the enzyme of water labeled with ^{18}O designated R_{H_2O} (eq 4). A proton from a donor group (BH) converts the zinc-bound ^{18}O-labeled hydroxide to zinc-bound $H_2{}^{18}O$, which readily exchanges with unlabeled water and is greatly diluted into the solvent water $H_2{}^{16}O$. The value of R_{H_2O} can be interpreted in terms of the rate constant from a predominant donor group to the zinc-bound hydroxide according to eq 6 (*25*), in which k_B is the rate constant for proton transfer to the zinc-bound hydroxide, K_B is the ionization constant for the donor group, and K_E is the ionization constant of the zinc-bound water molecule. For

our data, R_{H_2O}/[E] was determined by eq 6 using the program Enzfitter (Elsevier-Biosoft).

$$R_{H_2O}/[E] = k_B/\{(1 + K_B/[H^+])(1 + [H^+]/K_E)\} \quad (6)$$

For solvent hydrogen isotope effects, R_{H_2O}/[E] and k_{cat}/K_m were determined in 99.8% D_2O. All pH measurements are from uncorrected pH meter readings.

Inhibition. Inhibition by ethoxzolamide and acetazolamide was determined using ^{18}O exchange at chemical equilibrium. The values of K_i in Table 2 were obtained by least-squares fit of the catalytic velocity to the expression for competitive inhibition as a function of inhibitor concentration under the conditions that the total substrate concentration ($[CO_2] + [HCO_3^-] = 25$ mM) was much less than the apparent binding constant for total substrate, K_{eff}^S. At the pH of these measurements, 7.3−7.5, K_{eff}^S is greater than 100 mM for CA VII. The values of K_i determined from R_{H_2O} in the same manner agreed to within 25% with the values determined from R_1.

Hydrolysis of 4-Nitrophenyl Acetate. Measurement of the esterase function of rMCA VII was performed by the method of Verpoorte et al. (*26*) by following the absorbance change at 348 nm and the isosbestic point of 4-nitrophenol and its conjugate base, nitrophenolate ion. Concentrations of buffer and Na_2SO_4 were both 33 mM, and initial velocities were determined at 25 °C. The uncatalyzed rates were subtracted from the observed rates, and the kinetic constant k_{cat}/K_m and the determination of apparent ionization constants from the pH profile were carried out by nonlinear least-squares methods using Enzfitter (Elsevier-Biosoft).

RESULTS

Recombinant Murine CA VII. The full-length recombinant murine CA VII protein (rMCA VII) used in this study has a portion of its amino-terminal amino acid sequence derived from the human CA VII cDNA (*14*). More specifically, Ling et al. (*13*) obtained a 91% complete mouse CA VII cDNA by RT-PCR using RNA isolated from adult mouse (C57/BL6) brain. This cDNA lacked the sequence encoding the 28 amino-terminal residues. Lakkis et al. (*14*) then constructed an almost complete murine CA VII cDNA by carrying out PCR under relatively stringent conditions with a 5′ primer from the human CA VII sequence starting at the initial ATG and extending 26 nucleotides into the gene (*14*), and a 3′ primer determined by the murine CA VII cDNA of Ling et al. (*13*) (see Figure 1 for location of 5′ and 3′ primers). This construct allowed the determination of an additional 58 murine nucleotides after the 26 human 5′ primer nucleotides at the 5′ end of the murine CA VII cDNA (Figure 1). This extended murine CA VII cDNA sequence showed that 18 of the 19 newly derived amino acids are identical between human and murine CA VII (Figure 1). However, the rMCA VII cDNA used in this study has 26 nucleotides (including the start ATG) that are of human origin (Figure 1) and thus encodes a chimeric CA VII protein with the 9 N-terminal amino acids of human origin and the remaining 253 from the mouse. The nine amino-terminal residues of the murine CA VII protein remain unknown; however, in view of the highly conserved nature of the human and murine CA VII sequences, it is likely that they will be identical to the human sequence.

Catalytic Activity. The ratio k_{cat}/K_m for rMCA VII determined from ^{18}O exchange between CO_2 and water yielded a pH profile that was best fit by the sum of two ionizations (*27*), 6.2 ± 0.5 and 7.5 ± 0.3 (Figure 2, Table 1). A very similar result was obtained by stopped-flow spectrophotometry in which the pH profile of k_{cat}/K_m for CO_2 hydration over the pH range of 5.3−9.0 was also described by two ionizations with pK_a values of 6.2 ± 0.9 and 7.6 ± 0.5 and with a maximum of (3.3 ± 1.0) × 10^7 M^{-1} s^{-1} at high pH. The maximal values of k_{cat}/K_m for hydration measured by stopped-flow spectrophotometry were somewhat lower than those measured by ^{18}O exchange. The results of the steady-state measurements of k_{cat}/K_m in the HCO_3^- dehydration direction yielded a maximum at low pH and was dependent on a single ionizable group with pK_a of 6.8 ± 0.2 (Figure 2, Table 1). Because of the unfavorable equilibrium between CO_2 and HCO_3^-, we did not extend measurements in the dehydration direction to regions above pH 7.2. Hence, in the dehydration direction we did not observe the second ionization at a pH near 7.5.

We also measured the pH dependence of k_{cat}/K_m for two truncated forms of murine CA VII. One truncated form had the amino-terminal 23 residues removed, with a new amino terminus starting at the Pro 23 → Met mutation; it is designated MCA VIIb (Figure 1). MCA VIIb was further mutated by replacing His 64 with Ala. MCA VIIb had values of k_{cat}/K_m adequately fit to a single pK_a with values given in Table 1. The pH profile of k_{cat}/K_m for MCA VIIb H64A was identical.

Measurements of CO_2 hydration by stopped-flow spectrophotometry gave a maximum value of k_{cat} near 9.4 × 10^5 s^{-1} at pH >9 for rMCA VII (Figure 3, Table 1). Similar to the pH profile for k_{cat}/K_m, the data for k_{cat} over the pH range of 5.3−9 were best fit to two ionizations with corresponding pK_a values of 6.2 ± 0.2 and near 8.2 (Figure 3, Table 1). Steady-state measurements for k_{cat} for dehydration of HCO_3^- showed a maximum at low pH near 1.9 × 10^5 s^{-1} and a pK_a of 6.7 ± 0.1 (Figure 3, Table 1).

Values of the ^{18}O-exchange parameter R_{H_2O}/[E] describe the proton-transfer-dependent rate of exchange of $H_2{}^{18}O$ into solvent water (eq 4) (*23*). As was found for human CA II (*25*), for rMCA VII the pH profile of R_{H_2O}/[E] was bell-shaped with a maximum occurring near pH 7 (Figure 4). Reaction of carbonic anhydrase with acrolein results in formylethylation of exposed histidine, lysines, and possibly cysteine residues. The formylethylated rMCA VII was found to have maximal values of R_{H_2O}/[E] reduced by greater than 10-fold in the modified enzyme (Figure 4). R_{H_2O}/[E] for the unmodified rMCA VII was inhibited by $CuSO_4$ with an inhibition constant of 0.33 μM at pH 7.5 and 25 °C; $CuSO_4$ had no effect on the interconversion of CO_2 and HCO_3^- measured by R_1/[E] up to concentrations of $CuSO_4$ as great as 40 μM (data not shown).

The truncation mutants of murine CA VII had much reduced values of R_{H_2O}/[E] at pH <8 (Figure 5). The values of R_{H_2O}/[E] catalyzed by truncated mCA VIIb H64A were reduced even further in this region of pH (Figure 5). The inset of Figure 5 shows the pH profile for the differences in

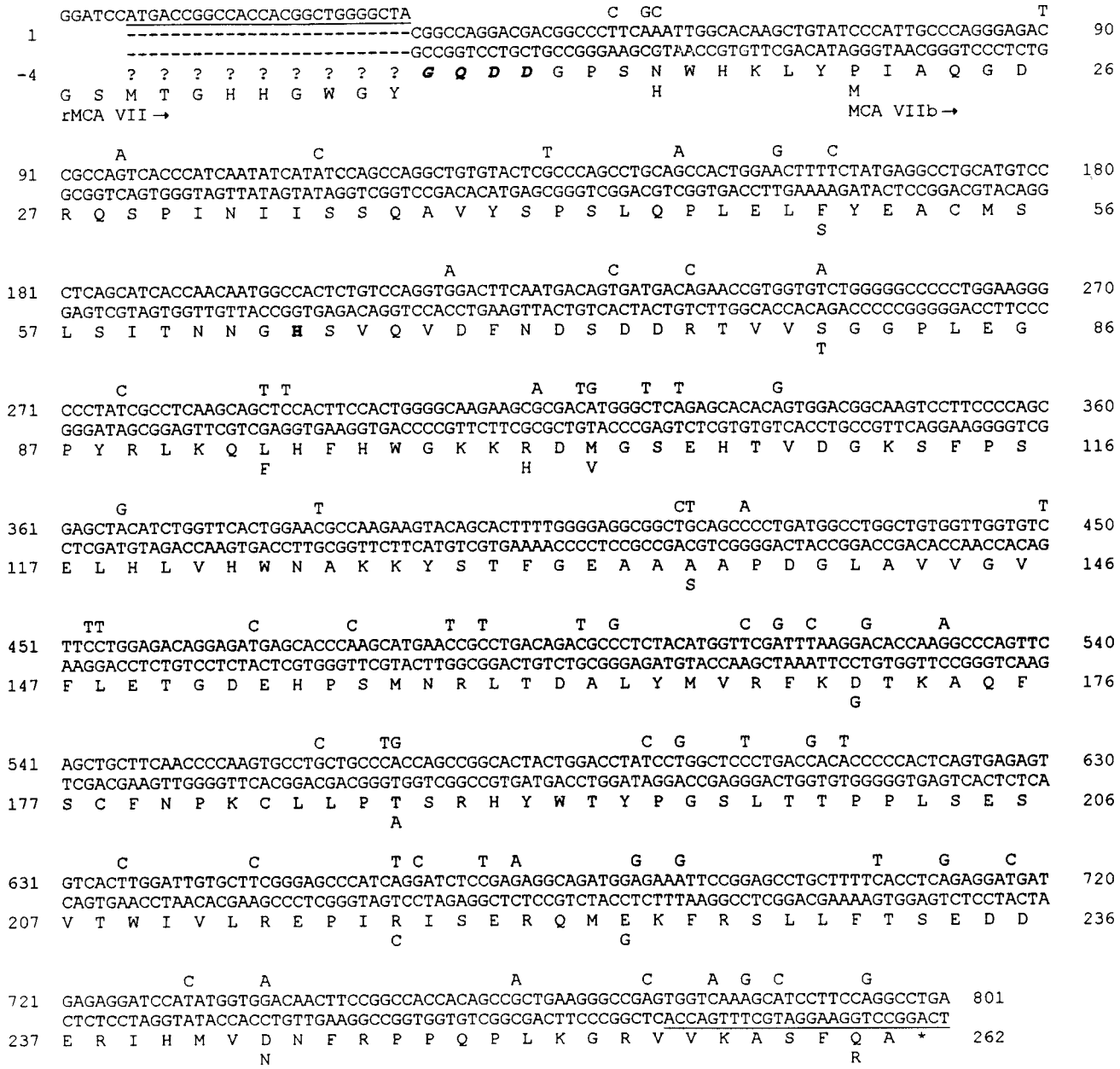

FIGURE 1: Sequence of MCA VII cDNA and derived amino acids. Differences from the human sequence (9) are indicated above and below the murine sequence. Numbering is based on the human CA I standard with the second N-terminal residue (Gly) as number 1. The four murine amino acids shown in boldface italic were confirmed by direct sequencing of the expressed recombinant murine CA VII protein (14). Underlined nucleotides identify the human and mouse primers used to amplify the recombinant MCA VII cDNA that expressed the full-length form of CA VII (rMCA VII →). The P23M mutation beginning the truncated MCA VII sequence is indicated (MCA VIIb →). His 64 is indicated in boldface type.

R_{H_2O}/[E] between the full-length rMCA VII and the truncated MCA VIIb, and between MCA VIIb and MCA VIIb H64A. The shapes of these two difference plots are very similar, reflecting in each case the loss of a proton donor or donors of pK_a near 6.9−7.5.

rMCA VII is able to catalyze the hydrolysis of 4-nitrophenyl acetate. The pH profile of k_{cat}/K_m has a maximum at pH > 9 of 71 M^{-1} s^{-1} and is best fit to two ionizations (Figure 6, Table 1) similar to k_{cat}/K_m in the CO_2 hydration direction. In some isozymes of carbonic anhydrase, there is a nonspecific esterase activity not associated with the zinc, as has been found in CA I (*28*) and CA III (*29*). However, that is not the case for rMCA VII; at a variety of different pH values, the esterase activity was found to be greater than 98% inhibited in the presence of equimolar concentrations of the active-site inhibitor ethoxzolamide (K_i = 0.5 nM) and enzyme (present at 10^{-7} M).

Inhibition of ^{18}O exchange between CO_2 and water catalyzed by rMCA VII with two the classic sulfonamides acetazolamide and ethoxzolamide was tested. The resulting values of the inhibition constant K_i are compared to the inhibition values of other isozymes of CA in Table 2.

The solvent hydrogen isotope effects (SHIE) observed for catalysis by rMCA VII were 1.0 ± 0.1 for k_{cat}/K_m for CO_2 hydration at pH 6.8. On k_{cat}, the SHIE was 3.0 ± 0.1 at pH 6.8 in solutions containing 25 mM Hepes, consistent with rate-determining proton transfer involving the aqueous ligand of the zinc (eq 2). The SHIE at pH 6.8 on R_{H_2O}/[E] was 3.3 ± 0.4.

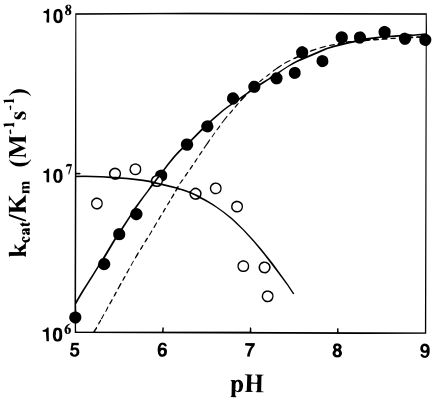

FIGURE 2: pH dependence of k_{cat}/K_m for (●) hydration of CO_2 and (○) dehydration of HCO_3^- catalyzed by rMCA VII at 25 °C. k_{cat}/K_m for hydration was obtained by ^{18}O exchange using solutions containing no buffers and in which the total ionic strength of the solution was maintained at 0.2 M by addition of Na_2SO_4 and the total concentration of all species of CO_2 was 25 mM. The solid line for CO_2 hydration is a nonlinear least-squares fit to two ionizations with values for the pK_a and maximal k_{cat}/K_m given in Table 1. The dashed line is a nonlinear least-squares fit to one ionization with a pK_a = 7.1 ± 0.1 and a maximal value of k_{cat}/K_m at (7.2 ± 0.3) × 10^7 M^{-1} s^1. The ratio k_{cat}/K_m for dehydration of HCO_3^- was obtained by stopped-flow spectrophotometry in the presence of 25 mM of one of the following buffers: pH 5.3−6.4, Mes; pH 6.6−7.2, Mops; pH 6.9−7.2, Hepes. The total ionic strength of the solution was maintained at 0.2 M with Na_2SO_4. The solid line for dehydration is a nonlinear least-squares fit to a single ionization with pK_a and maximal k_{cat}/K_m given in Table 1.

DISCUSSION

Comparison of Isozymes of Carbonic Anhydrase. We have compared the steady-state catalytic constants of CA VII with CA II, the most efficient of the carbonic anhydrase isozymes, and with five other isozymes in the α-class of the carbonic anhydrases. The steady-state constant k_{cat}/K_m contains the rate constants up to and including the first irreversible step, which is the departure of HCO_3^-; these are the steps of eq 1. The pH dependence of k_{cat}/K_m describes the ionization state of the zinc-bound water (*2*, *3*). In the CO_2 hydration direction, the maximal value of k_{cat}/K_m of 7.6 × 10^7 M^{-1} s^{-1} for rMCA VII at high pH is half that of CA II but somewhat greater than those for CA I, CA IV, and CA V (Table 3). We observed a solvent hydrogen isotope effect of 1.0 ± 0.1 on k_{cat}/K_m, indicating no rate-contributing proton transfer in the steps of eq 1 and consistent with a direct nucleophilic attack of the zinc-bound hydroxide on CO_2 (*2*); in this respect, rMCA VII is similar to CA II and the other isozymes in the α-class. We also point out that the maximal value of k_{cat}/K_m is the same for rMCA VII and for the truncation mutant MCA VIIb (Table 1). Thus, the amino terminus has no role in the steps of eq 1, the catalysis by CA VII of the conversion of CO_2 into bicarbonate at the zinc.

The maximal value of the turnover number k_{cat} for hydration of CO_2 catalyzed by rMCA VII approaches that of CA II (Table 3). The value of k_{cat} contains rate constants for the steps from the enzyme−substrate complex through the proton transfers of eq 2. The kinetic constants for rMCA VII place it among the most efficient of the carbonic anhydrases with 67% of the activity of CA II. Considering the similarity in the steady-state constants for CO_2 hydration catalyzed by rMCA VII and CA II, it is interesting that the capacity of rMCA VII to catalyze the hydrolysis of 4-nitrophenyl acetate (maximal k_{cat}/K_m = 71 M^{-1} s^{-1}; Figure 6, Table 1) is much less than that of human CA II [maximal k_{cat}/K_m = 3 × 10^3 M^{-1} s^{-1}; (*4*)].

Proton Transfer in CA VII. Several results suggest that His 64 is the predominant proton shuttle in CA VII, as it is in CA II. First, there is no other residue in the active-site cavity which is a likely shuttle of pK_a near 7. Second, inhibition by $CuSO_4$ of ^{18}O exchange catalyzed by rMCA VII shows properties very similar to those observed for inhibition by $CuSO_4$ of human CA II in which His 64 is a proton shuttle (*30*). In HCA II, cupric ion coordinates to the imidazole side chain of His 64 and blocks the proton transfer role of this residue (*31*). This results in inhibition of R_{H_2O}/[E] which is dependent on proton transfer, but has no effect on R_1/[E] which measures interconversion of CO_2 and HCO_3^- in the first stage of catalysis (eq 3). The same pattern is seen for rMCA VII. And third, chemical modification of rMCA VII by acrolein also is consistent with patterns observed in CA II (*22*, *32*). This treatment formylethylates exposed histidines and lysines and possibly cysteines; however, the prominent effect in CA II is the alkylation of His 64 resulting in reduction of the proton shuttle function of this residue (*32*). This also is observed in rMCA VII and is shown in Figure 4 in which the decrease in R_{H_2O}/[E] with the modified enzyme is apparent. The inset of Figure 4 gives the difference in R_{H_2O}/[E] between unmodified and modified enzymes and shows that the modification has resulted in the elimination of the proton shuttle capacity of a group (or groups) of pK_a 7.4 ± 0.1. Finally, the pH profile for rMCA VII in Figure 4 is nearly identical with that of human CA II, and in the case of CA II replacement of His 64 by Ala showed that His 64 is the predominant proton shuttle (*5*).

Effect of the Amino-Terminal Residues. We have observed no difference in k_{cat}/K_m for hydration between the rMCA VII and the truncation mutant MCA VIIb. Thus, the truncation is not affecting the catalysis of the interconversion of CO_2 and bicarbonate at the zinc (eq 1). However, two results suggest that the truncation is affecting proton transfer: the 2-fold decrease observed at pH 9.1 in k_{cat} for hydration compared with full length (Table 1), and the decrease by an order of magnitude in R_{H_2O}/[E] near pH 6 (Figure 5). Aronsson et al. (*33*) observed catalysis by a truncated variant of human CA II in which 20 residues at the amino terminus were removed; it had an overall CO_2 hydration activity 15% of wild-type human CA II.

Thus, it is a reasonable assumption that the truncation of the amino-terminal 23 residues has decreased the ability of His 64 to function as a proton shuttle. This suggestion is supported by the difference between the pH profile for R_{H_2O}/[E] for rMCA VII and for MCA VIIb shown in the inset in Figure 5. This difference plot shows the bell-shaped pH dependence consistent with the loss of a single proton shuttle of pK_a 6.9 ± 0.2, and corresponding to a loss in proton-transfer capacity (R_{H_2O}/[E]) of 3.4 × 10^5 s^{-1} upon truncation. By this argument, the small maximum near pH 6 in the pH profile for the MCA VIIb is due to the reduced capacity of His 64 to act as a proton shuttle (Figure 5). This is apparent from the pH dependence of the H64A MCA VIIb mutant (Figure 5). The difference in values of R_{H_2O}/[E] for MCA VIIb and H64A MCA VIIb is also given in the inset in Figure

Table 1: Catalysis by Carbonic Anhydrase VII: Maximal Values of Steady-State Constants with Values of Apparent pK_a[a]

	k_{cat}/K_m (M^{-1} s^{-1})	pK_a	k_{cat} (s^{-1})	pK_a
hydration of CO_2	$(7.6 \pm 0.3) \times 10^7$	6.2 ± 0.5 7.5 ± 0.3	$(9.4 \pm 2.4) \times 10^5$	~8.2[b] 6.2 ± 0.2
hydration of CO_2 (MCA VIIb)[c]	$(8.2 \pm 0.3) \times 10^7$	7.7 ± 0.1	$(4.5 \pm 0.4) \times 10^5$	–[d]
dehydration of HCO_3^-	$(9.7 \pm 1.0) \times 10^6$	6.8 ± 0.2	$(1.9 \pm 0.1) \times 10^5$	6.7 ± 0.1
hydrolysis of 4-nitrophenyl acetate	71 ± 8	5.3 ± 0.3 7.1 ± 0.1		
hydration of CO_2 by acrolein-modified enzyme	$(2.7 \pm 0.1) \times 10^7$	6.7 ± 0.1	$(4.0 \pm 0.9) \times 10^4$	8.8 ± 0.2 5.8 ± 0.2

[a] All data were obtained using rMCA VII protein except where indicated. Experimental conditions as given in the corresponding figure legends. [b] Because of the uncertainty in the maximal value of k_{cat}, this pK_a is poorly determined. [c] This truncated form of murine CA VII is lacking the amino-terminal 23 residues of rMCA VII shown in Figure 1. [d] Not measured. The maximal value of k_{cat} was measured at pH 9.1.

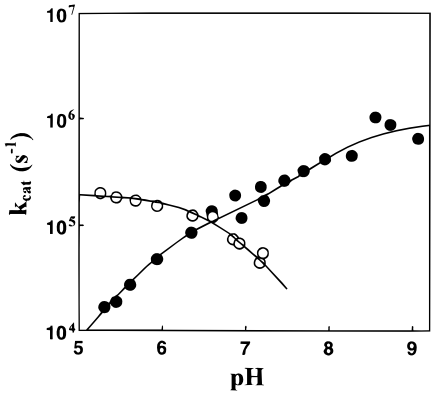

FIGURE 3: Turnover number k_{cat} for (●) hydration of CO_2 and (○) dehydration of HCO_3^- catalyzed by rMCA VII, both obtained by stopped-flow spectrophotometry at 25 °C in the presence of 25 mM of one of the following buffers: pH 5.3−6.4, Mes; pH 6.6−7.2, Mops; pH 6.9−7.5, Hepes; pH 7.7−8.3, Taps; pH 8.6−9.1, Ches. The total ionic strength of solution was maintained at 0.2 M with Na_2SO_4. The solid lines are nonlinear least-squares fits to two ionizations for the hydration of CO_2 and one ionization for the dehydration of HCO_3^- with pK_a values and maximal k_{cat} given in Table 1.

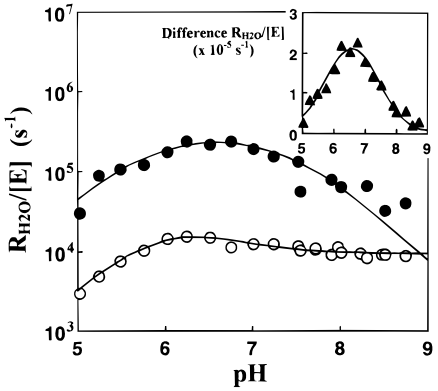

FIGURE 4: (●) Variation with pH of $R_{H_2O}/[E]$, the proton-transfer-dependent rate constant for the release from the enzyme of ^{18}O-labeled water catalyzed by rMCA VII. Solutions contained no buffers, and the total ionic strength of the solution was maintained at 0.2 M by addition of Na_2SO_4; the total concentration of all species of CO_2 was 25 mM. The solid line is a fit of eq 6 to the data with values of the pK_a for the proton donor of 7.4 ± 0.1 and acceptor groups of 5.8 ± 0.1 and $k_B = (3.2 \pm 0.4) \times 10^5$ s^{-1}. (○) Variation with pH of $R_{H_2O}/[E]$ catalyzed by the acrolein-modified rMCA VII under the same conditions. (Inset) Difference in $R_{H_2O}/[E]$ between the unmodified and acrolein-modified rMCA VII. The solid line is a nonlinear least-squares fit describing proton transfer (eq 6) from a donor group of pK_a 7.4 ± 0.1 and zinc-bound hydroxide, the conjugate acid of which has pK_a 5.8 ± 0.1 with a rate constant for proton transfer $k_B = (2.8 \pm 0.3) \times 10^5$ s^{-1}.

5. Here again, the data are consistent with the loss of a single proton donor of pK_a 7.5 ± 0.2 corresponding now to a smaller loss in proton-transfer capacity of 5×10^4 s^{-1}.

By this explanation, the proton shuttle capacity of His 64 is lessened by removal of the amino-terminal 23 residues of rMCA VII. There are several possibilities for this loss. The first is a conformational change of MCA VIIb in which His 64 is at a distance less effective for proton transfer or in which His 64 has a broader range of side-chain conformations than in the full-length enzyme and hence spends less time in the conformations appropriate for proton transfer. It is also possible that the 3 histidines of the amino-terminal 23 residues (Figure 1) are significant secondary proton donors in rMCA VII. We consider this unlikely because based on the structure of CA II (*34*) the distance of these residues from the zinc (>18 Å) is much greater than for His 64 (~7 Å); moreover, it is His 64 that has been shown to play the predominant role as proton shuttle in the well-studied catalysis by CA II which has catalytic properties very similar to those of rMCA VII as discussed above. In support of the suggestion that the amino-terminal end of rMCA VII influences the function of His 64 as proton shuttle, we point out that deletions of amino-terminal residues of carbonic anhydrases that lack an effective proton shuttle at position 64, namely, CA III[2] and CA V (*21*), show catalytic properties nearly identical with their full-length counterparts. This topic is under further study.

Assignment of pK_a Values. The pH dependence of k_{cat}/K_m in the CO_2 hydration direction can be described by two ionizations for rMCA VII, near pK_a 6.2 and 7.5 (Figure 2, Table 1). The pH-rate profile for the esterase activity of rMCA VII also appears dependent on two ionizations with similar values of pK_a (Figure 6, Table 1). The bell-shaped pH profiles typically found for R_{H_2O} can be described by eq 6 which expresses $R_{H_2O}/[E]$ as the product of the protonated form of the donor group and the unprotonated form of the aqueous ligand of the zinc (*25*). By this analysis, the data of Figure 4 for unmodified rMCA VII demonstrate two values of pK_a, near 5.8 and 7.4, which again suggest the same ionizations as observed in k_{cat}/K_m for CO_2 hydration and hydrolysis of 4-nitrophenyl acetate (Table 1). One of these ionizations is clearly that of the zinc-bound water; the

[2] A. Hevia, C. K. Tu, D. N. Silverman, and P. J. Laipis, unpublished observations.

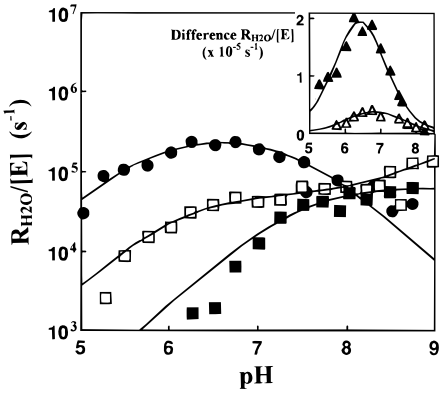

FIGURE 5: Variation with pH of R_{H_2O}/[E] catalyzed by (●) full-length rMCA VII, (□) the truncated MCA VIIb (see Figure 1), and (■) a H64A mutant of MCA VIIb. Experimental conditions as in Figure 4. Inset: (▲) The difference in R_{H_2O}/[E] between rMCA VII and MCA VIIb. The solid line is a nonlinear least-squares fit describing proton transfer (eq 6) from a donor group of pK_a 6.9 ± 0.2 and zinc-bound hydroxide, the conjugate acid of which has pK_a 5.9 ± 0.2 with a rate constant for proton transfer of $k_B = (3.4 \pm 0.8) \times 10^5$ s^{-1}. (△) The difference in R_{H_2O}/[E] between MCA VIIb and the H64A mutant of MCA VIIb. The solid line is a nonlinear least-squares fit describing proton transfer (eq 6) from a donor group of pK_a 7.5 ± 0.2 and zinc-bound hydroxide, the conjugate acid of which has pK_a 6.2 ± 0.2 with a rate constant for proton transfer of $k_B = (5.5 \pm 1.1) \times 10^4$ s^{-1}.

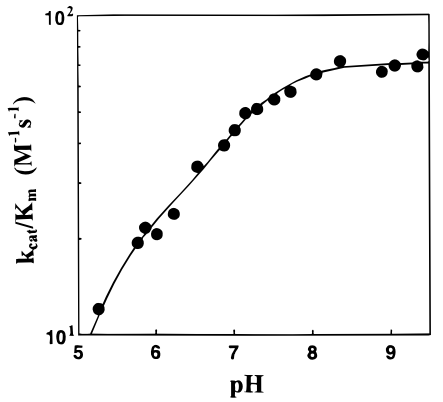

FIGURE 6: pH dependence of k_{cat}/K_m for the hydrolysis of 4-nitrophenyl acetate catalyzed by rMCA VII. Data were obtained at 25 °C in 33 mM of one of the following buffers: pH 5.3−6.5, Mes; pH 6.9−7.2, Mops; pH 7.3−7.7, Hepes; pH 8.1−8.9, Taps; pH 9.1−9.4, Ches. The solid line is a nonlinear least-squares fit of two ionizations with pK_a values and maximal k_{cat}/K_m given in Table 1.

Table 2: Inhibition Constants, K_i (Nanomolar), for Isozymes of Carbonic Anhydrase Determined by ^{18}O Exchange[a]

isozyme	K_i (nM) acetazolamide	ethoxzolamide	reference
human CA II	60	8	*40*
human CA III	40000	8000	*40*
murine CA IV	−	16	*15*
murine CA V	60	5	*22*
murine CA VII	16	0.5	this work

[a] All values of K_i were determined at pH 7.2−7.5 and 25 °C.

other ionization most likely results from a perturbation of the pK_a of the zinc-bound water caused by the electrostatic interaction of a nearby group. Perturbations of the pK_a of the zinc-bound water have been described for mutants of CA. For example, in human CA II, the introduction of a glutamate in the active site changes the pH dependence of k_{cat}/K_m for ester hydrolysis from a single ionization to one described by two ionizations (*35*). Also, Simonsson et al. (*36*) observed a perturbation of the apparent pK_a of k_{cat}/K_m for the esterase function catalyzed by CA II at low ionic strength and attributed it to His 64.

Table 3: Maximal Values of the Steady-State Constants for CO_2 Hydration Catalyzed by Isozymes of Carbonic Anhydrase in the α-Class[a]

isozyme	k_{cat} ($\times 10^{-5}$ s^{-1})	k_{cat}/K_m ($\times 10^{-7}$ M^{-1} s^{-1})	reference
human CA I	2	5	*6*
human CA II	14	15	*6*
human CA III	0.1	0.03	*41*
murine CA IV	11	3.2	*15*
murine CA V	3	3.0	*22*
rat CA VI[b]	0.7	1.6	*42*
murine CA VII	9.4	7.6	this work

[a] Data obtained at 25 °C. [b] Data obtained at pH 7.5 probably do not represent maximal values.

By the principle of kinetic equivalence (*37*, *38*), it is not possible to assign these values of pK_a without further information. By comparison of the data from our steady-state measurements and ^{18}O exchange, we have been able to achieve an assignment. The ^{18}O-exchange data of Figure 4 taken alone are equally consistent with the following two assignments: (1) The pK_a of 7.4 is the zinc-bound water, and the pK_a of 5.8 is His 64 with $k_B = (1.3 \pm 0.4) \times 10^7$ s^{-1} for the rate constant for intramolecular proton transfer in the dehydration direction (as shown for ^{18}O exchange in eq 4); (2) the pK_a of 7.4 is for His 64, and the pK_a of 5.8 is the zinc-bound water in which case $k_B = (3.2 \pm 0.4) \times 10^5$ s^{-1}. It is helpful to compare the ^{18}O-exchange data with the steady-state turnover for dehydration. Like k_B, the turnover number for dehydration, k_{cat}, is dependent on proton transfer to the zinc-bound hydroxide. The maximal value of k_{cat} for dehydration catalyzed by rMCA VII was 2×10^5 s^{-1} (Table 1), a value consistent with assigning the pK_a near 7.4 to His 64 and the pK_a near 5.8 to the zinc-bound water.

However, for hydration of CO_2, the pH profile for k_{cat} is less clear (Figure 3); the pH profile of k_{cat} for hydration of CO_2 catalyzed by rMCA VII is also described by two ionizations, one with a pK_a near 6.2 ± 0.2 and one with a poorly determined pK_a near 8.2 (Figure 3, Table 1). These observations in rMCA VII of two ionizations influencing the k_{cat} for hydration are very similar to the observations of Hurt et al. (*15*) in which the k_{cat} for murine CA IV was found to depend on two ionizations. One of these had an apparent pK_a of 6.3 and was assigned to His 64, and a second with pK_a of 9.1 may represent proton transfer to basic residues more distant from the zinc than His 64; this result is observed for many other isozymes of carbonic anhydrase (*39*). The observed apparent pK_a of 6.2 for the proton donor does not agree with our assignment of pK_a values for k_{cat}/K_m and R_{H_2O} described above. Perhaps the pH profile for k_{cat} is too complicated to be described by two ionizations. Moreover, the analysis of the data for k_{cat} may be complicated by a role for the external buffer as proton donor, which is not a consideration for interpretation of k_{cat}/K_m and R_{H_2O}.

Inhibition. The inhibition of rMCA VII by the sulfonamides acetazolamide and ethoxzolamide measured by ^{18}O

exchange is greater than for the other isozymes (Table 2). These sulfonamide inhibitors are expected to bind directly to the zinc and adhere to the hydrophobic side of the active-site cavity as demonstrated in human CA II (*34*). Many of the residues implicated in sulfonamide binding with CA II are conserved in rMCA VII. Two exceptions are L204 and C206 in CA II which in murine CA VII are serines.

Conclusions. Murine CA VII is a very efficient carbonic anhydrase with catalytic activity similar to the most active of the isozymes in the α class. Moreover, among these isozymes it is the most inhibitable by two widely used sulfonamides when measured by ^{18}O exchange. Unique among the other wild-type isozymes of the α class, CA VII demonstrates the effect of two ionizations in the pH profile of k_{cat}/K_m. One of these is the ionization of the zinc-bound water (pK_a 6.2), and the second is suggested to be His 64 (pK_a 7.5) based on inhibition by $CuSO_4$ and acrolein and in analogy with the other most active isozymes in this class, CA II and CA IV. The assignment of these values of pK_a was done by a novel application of ^{18}O-exchange rates. Moreover, we have shown that the amino-terminal end of carbonic anhydrase has a role in enhancing proton transfer in catalysis.

ACKNOWLEDGMENT

We thank Bret Schipper for laboratory technical assistance. We are also grateful to Kaile Adney and Nina Wadhwa for assistance with the recombinant enzymes.

REFERENCES

1. Hewett-Emmett, D., and Tashian, R. E. (1996) *Mol. Phylogenet. Evol. 5*, 50−77.
2. Lindskog, S. (1997) *Pharm. Ther. 74*, 1−20.
3. Christianson, D. W., and Fierke, C. A. (1996) *Acc. Chem. Res. 29*, 331−339.
4. Steiner, H., Jonsson, B.-H., and Lindskog, S. (1975) *Eur. J. Biochem. 59*, 253−259.
5. Tu, C. K., Silverman, D. N., Forsman, C., Jonsson, B.-H., and Lindskog, S. (1989) *Biochemistry 28*, 7913−7918.
6. Khalifah, R. G. (1971) *J. Biol. Chem. 246*, 2561−2573.
7. Lindskog, S. (1984) *J. Mol. Catal. 23*, 357−368.
8. Rowlett, R. S. (1984) *J. Protein Chem. 3*, 369−393.
9. Montgomery, J. C., Venta, P. J., Eddy, R. L., Fukushima, Y. S., Shows, T. B., and Tashian, R. E. (1991) *Genomics 11*, 835−848.
10. Nagao, Y., Platero, J. S., Waheed, A., and Sly, W. S. (1993) *Proc. Natl. Acad. Sci. U.S.A. 90*, 7623−7627.
11. Ling, B., Bergenhem, N. C. H., Dodgson, S. J., Forster, R. E., and Tashian, R. E. (1994) *Isozyme Bull. 27*, 47.
12. Lakkis, M. M., O'Shea, K. S., and Tashian, R. E. (1997) *J. Histochem. Cytochem. 45*, 657−662.
13. Ling, B., Bergenhem, N. C. H., and Tashian, R. E. (1995) *Isozyme Bull. 28*, 32.
14. Lakkis, M. M., Bergenhem, N. C. H., and Tashian, R. E. (1996) *Biochem. Biophys. Res. Commun. 226*, 268−272.
15. Hurt, J. D., Tu, C. K., Laipis, P. J., and Silverman, D. N. (1997) *J. Biol. Chem. 272*, 13512−13518.
16. Guan, K. L., and Dixon, J. E. (1991) *Anal. Biochem. 192*, 262−267.
17. Smith, D. B., and Johnson, K. J. (1988) *Gene 67*, 31−40.
18. Khalifah, R. G., Stader, D. J., Bryant, S. H., and Gibson, S. M. (1977) *Biochemistry 16*, 2241−2247.
19. Kunkel, T. A., Roberts, J. D., and Zakour, R. A. (1987) *Methods Enzymol. 154*, 367−382.
20. Tanhauser, S. M., Jewell, D. A., Tu, C. K., Silverman, D. N., and Laipis, P. J. (1992) *Gene 117*, 113−117.
21. Heck, R. W., Tanhauser, S. M., Manda, R., Tu, C. K., Laipis, P. J., and Silverman, D. N. (1994) *J. Biol.* Chem. *269*, 24742−24746.
22. Pocker, Y., and Janjic, N. (1988) *J. Biol. Chem. 263*, 6169−6176.
23. Silverman, D. N. (1982) *Methods Enzymol. 87*, 732−752.
24. Simonsson, I., Jonsson, B.-H., and Lindskog, S. (1979) *Eur. J. Biochem. 93*, 409−417.
25. Silverman, D. N., Tu, C. K., Chen, X., Tanhauser, S. M., Kresge, A. J., and Laipis, P. J. (1993) *Biochemistry 32*, 10757−10762.
26. Verpoorte, J. A., Mehta, S., and Edsale, J. T. (1967) *J. Biol. Chem. 242*, 4221−4229.
27. Tipton, K. F., and Dixon, H. B. F. (1979) *Methods Enzymol. 63*, 183−234.
28. Wells, J. W., Kandel, S. I., Kandel, M., and Gornall, A. G. (1975) *J. Biol. Chem. 250*, 3522−3530.
29. Tu, C. K., Thomas, H. G., Wynns, G. C., and Silverman, D. N. (1986) *J. Biol. Chem. 261*, 10100−10103.
30. Tu, C. K., Wynns, G. C., and Silverman, D. N. (1981) *J. Biol. Chem. 256*, 9466−9470.
31. Eriksson, A. E., Jones, T. A., and Liljas, A. (1986) in *Zinc Enzymes* (Bertini, I., Luchinat, C., Maret, W., and Zeppezauer, M., Eds.) pp 317−328, Birkhauser, Boston.
32. Tu, C. K., Wynns, G. C., and Silverman, D. N. (1989) *J. Biol. Chem. 264*, 12389−12393.
33. Aronsson, G., Mårtensson, L.-G., Carlsson, U., and Jonsson, B.-H. (1995) *Biochemistry 34*, 2153−2162.
34. Eriksson, A. E., Kylsten, P. M., Jones, T. A., and Liljas, A. (1988) *Proteins: Struct., Funct., Genet. 4*, 283−293.
35. Forsman, C., Behravan, G., Jonsson, B.-H., Liang, Z. W., Lindskog, S., Ren, X., Sandström, J., and Wallgren, K. (1988) *FEBS Lett. 229*, 360−362.
36. Simonsson, I., Jonsson, B.-H., and Lindskog, S. (1982) *Eur. J. Biochem. 123*, 29−36.
37. Fersht, A. (1985) in *Enzyme Structure and Mechanism*, pp 90−92, W. H. Freeman and Co., New York.
38. Jencks, W. P. (1969) in *Catalysis in Chemistry and Enzymology*, pp 221−222, McGraw-Hill Book Co., New York.
39. Earnhardt, J. N., Qian, M. Z., Tu, C. K., Laipis, P. J., and Silverman, D. N. (1998) *Biochemistry 37*, 7649−7655.
40. LoGrasso, P. V., Tu, C. K., Jewell, D. A., Wynns, G. C., Laipis, P. J., and Silverman, D. N. (1991) *Biochemistry 30*, 8463−8470.
41. Jewell, D. A., Tu, C. K., Paranawithana, S. R., Tanhauser, S. M., LoGrasso, P. V., Laipis, P. J., and Silverman, D. N. (1991) *Biochemistry 30*, 1484−1490.
42. Feldstein, J. B., and Silverman, D. N. (1984) *J. Biol. Chem. 259*, 5447−5453.

BI980046T